Multilayered microcoils for microactuators and characterization of their operational limits in body-like environments

Efren Diez-Jimenez, Ignacio Valiente-Blanco, Gabriel Villalba-Alumbreros, Miguel Fernandez-Munoz, Diego Lopez-Pascual, Alberto Lastra-Sedano, Carlos Moron-Alguacil, Alba Martinez-Perez

***Abstract* - Multilayered microcoils are of great importance for the development of advanced electromagnetic microactuators and especially important to develop high sensitivity microsensors and magnetic field neural stimulators for medical applications. A clean room-free procedure for manufacturing multilayered micrometric coils is presented in this work. The production of miniaturized multilayered coils from tens to hundreds of micrometres long is demonstrated. The microcoils have outer diameters ranging between 150 and 300 µm, arrangements of up to 5 consecutive layers, and an average fill factor of 85%. This means 3 times smaller diameters than the smallest diameter ever achieved by winding techniques while keeping a high fill factor and a large number of layers. Such small and highly performant microcoils have never been demonstrated neither by winding processes nor epitaxial growth techniques. These microcoils were tested inside different human body-like environments. Maximum current density vs. temperature was measured in air, fat tissue, muscle tissue and simulated body fluid at 36 °C. A maximum current density of 3600 A/m^2 has been measured before coil failure. Experiments demonstrated that current densities up to 610 A/m^2 can safely be supplied to coils without risk of harm to internal tissues. These counterintuitive values are orders of magnitude larger than typical current densities used in macroscale actuators windings.** [1]

***Index terms* - microsolenoids, microcoils, MEMS, microactuators, solenoids, bio-microdevice, inductors MRI sensors**

I. Introduction

Microcoils and microwindings are of great importance in many miniaturized applications. Microelectromechanical systems (MEMS) [1], microactuators [2]–[4] and microgenerators, frequently use microcoils for generating alternating magnetic fields that create motion [5], [6]. Microcoils are also a key component of wireless power transmission (WPT) devices [7] and communication microantennas [8]. Microinductors mainly created by microcoils are basic passive elements of microelectronics.

More specifically, microcoils are also widely used in medical devices, e.g., in magnetic resonance imaging (MRI) microcoils are used to retrieve the signal response by magnetic flux measurements [9]. Moreover, they are an essential part of a wide variety of implantable medical devices (IMDs) and insertable medical applications (IMAs), such as actuators [10], antennas [11], WPT systems and sensors [12], [13], microrobots [14]–[16] ablation systems [17] and biosensors [18]–[20]. In biomedical applications such as ablation or heating, the function of microcoils is to generate heat through Joule heating effect. In neurostimulators, microcoils are used to create magnetic and electric fields to stimulate brain zones. More significantly, for microactuators, microcoils are used to induce magnetic fields to create force / torque.

Two main micromanufacturing techniques can be found for microcoils: material deposition techniques, like UV-LIGA, and wire winding processes. The UV-LIGA method can be applied to create multilayered microcoils. Single-layer multiturn microcoils can be created very efficiently and relatively simply, as the 2D feature size can be very small, even smaller than 10 µm [21]–[23]. These lithography-plating methods require complex and expensive clean room facilities and many manufacturing steps. Another important drawback is that the fill factor of the coil is never larger than 50% in the best of cases. Additionally, high-performing soft magnetic materials, like FeCo alloys, are complex to deposit, drastically limiting the induction/sensing performance of microcoils.

An alternative technique is to directly wind thin copper wires around micrometric ferromagnetic cores. Microcoils in the range of 1-2 mm long and diameters down to 0.5 mm have been successfully wound [24], [25]. Commercial companies can supply microcoils with diameters down to 0.5 mm [26], [27]. Fill factors reported for those previous references are as high as 70% - 85%. Other relevant works related to microcoils manufacturing based on 3D printing and alternatives techniques can be found in references [28]–[30].

In a first part of this work, a novel semiautomatic manufacturing method for multilayered microcoils

[D]ate ---

This research was supported by the European Union's Horizon 2020 research and innovation programme under grant agreement No 857654–UWIPOM2. In addition, this work was partially supported by the Spanish Ministry of Science, Innovation and Universities under Ramón & Cajal Research Grant number RYC-2017-23684.

Corresponding author: E. Diez-Jimenez, email: efren.diez@uah.es. E. Diez-Jimenez, Ignacio Valiente Blanco, Miguel Fernandez-Munoz and Gabriel Villalba-Alumbreros, Diego Lopez-Pascual, Carlos Moron-Alguacil, Alba Martinez-Perez are with the Mechanical Engineering Area of Universidad de Alcalá, Cta Madrid-Barcelona km 33.6, 28805, Alcalá de Henares, Spain.

Email: efren.diez@uah.es, i.valiente@uah.es, gabriel.villalba@uah.es, miguel.fernandezmuno@uah.es, d.lopezp@uah.es , carlos.moron@uah.es, alba.martinezperez@uah.es, Alberto Lastra-Sedano is with the Physics and Mathematics Department of Universidad de Alcalá, Cta Madrid-Barcelona km 33.6, 28805, Alcalá de Henares, Spain. Email: alberto.lastra@uah.es

The next additional items have been submitted as supplementary information:

- Video explaining steps of the manufacturing process.
- Video of the thermoelectrical test of the microcoils in air
- Video of the thermoelectrical test of the microcoils in SBF.
- CAD model of the winding system.

This article has been accepted for publication in IEEE/ASME Transactions on Mechatronics. This is the author's version which has not been fully edited and content may change prior to final publication. Citation information: DOI 10.1109/TMECH.2022.3215233

manufacturing is presented. This technique allows to create much smaller multilayered microcoils than previously achieved. It is based on winding techniques with some key adaptations that permits further miniaturization of the coils. We produced multilayered microcoils approximately 500 µm long with outer diameters between 150 and 300 µm, 3 times smaller than the smallest diameter ever achieved, as far as we are concerned, while keeping a high fill factor. A total of 125 turns in up to 5 consecutive layers were achieved with a high wire fill factor of 85% (epitaxial techniques can only reach around 50% of fill factor). This combination of parameters: micrometric diameter and length, multiple layers and a high fill factor has no precedent in literature.

The second part of this work presents a characterization of the operational thermoelectrical limits of the manufactured microcoils inside human-body-like environments. Previous works in the literature have reported the current density limits of coils manufactured by different techniques, but always from the perspective of component failure. Under these considerations, maximum current densities up to 5800 A/mm^2 were reported for on-substrate PCB integrated single-layer microcoils [31]. In another study, a maximum current density of 250 A/mm^2 was reported for microcoils on a silicon wafer operating in an air environment [32]. For internal medical applications, the microcoil temperature should be limited to 43 °C to avoid tissue damage [33]. In this paper, the maximum current limits of microcoils in body-like operational conditions is presented for the first time.

II. Multilayered Microcoil Manufacturing

The generated magnetic field inside a coil or a solenoid, i.e. in the core, depends on the number of turns, circulating current and the magnetic permeability of the core, which are directly linked to current density through wires. The maximum allowable current density depends on the heat dissipation capacity of the surrounding environment. The magnetic field inside an infinitely long solenoid can be expressed as:

$$B = \frac{\mu n I}{l} = \mu j b F = \mu j c d F \quad (1)$$

Where µ is the absolute magnetic permeability, n is the number of turns, I is the current, j is current density, l is the length, c is number of layers, b is thickness of the solenoid, F is fill factor (which depends on the geometrical distribution of the wires) and d is diameter of wires. Therefore, to maximize the inducing magnetic field inside the solenoid, increasing the number of layers (c) and the fill factor (F) turns out to be critical. The manufacturing method has been adjusted to maximize number of layers and fill factor in micrometric sizes.

A. Materials and method

The proposed winding method produces an organized helical winding. Wires are placed helically in every layer. Following the direction of rotation during the winding, from layer to layer, alternating between right-hand and left-hand, the wires cross and locate above the layer underneath.

The magnetic wire selected for this application is HSP15 Solabond from Elektrisola (Reichshof-Eckenhagen, Germany). This wire is a 20 µm diameter self-bonding enamelled copper wire with a 2 µm thick base coat made of polyurethane, plus a 2 µm thick extra layer of bond coat made of polyamide. All coatings are biocompatible materials. The inner core can be made of any material, provided it is stiff enough to withstand the wire tension. All microcoils reported in this paper are manufactured using a 100 µm diameter stainless steel 304 pin as the inner core, as shown in Fig 1-a.

The microwinding machine is shown in Fig 1-b. This machine is designed for semiautomatic operation, controlled by one person. It can produce a 4-layer microcoil in less than 7 min. The copper wire reel is placed in a baseplate with an attached post where a mechanical tensioner provides control on the wire. Heat flows were basically on/off operation, which can also be programmed using triggering functions. The mechanical tensioner is the YMH-00 model from Tailkuke (China). Adequate tension for the selected wire is experimentally found and defined as 2.5 cN.

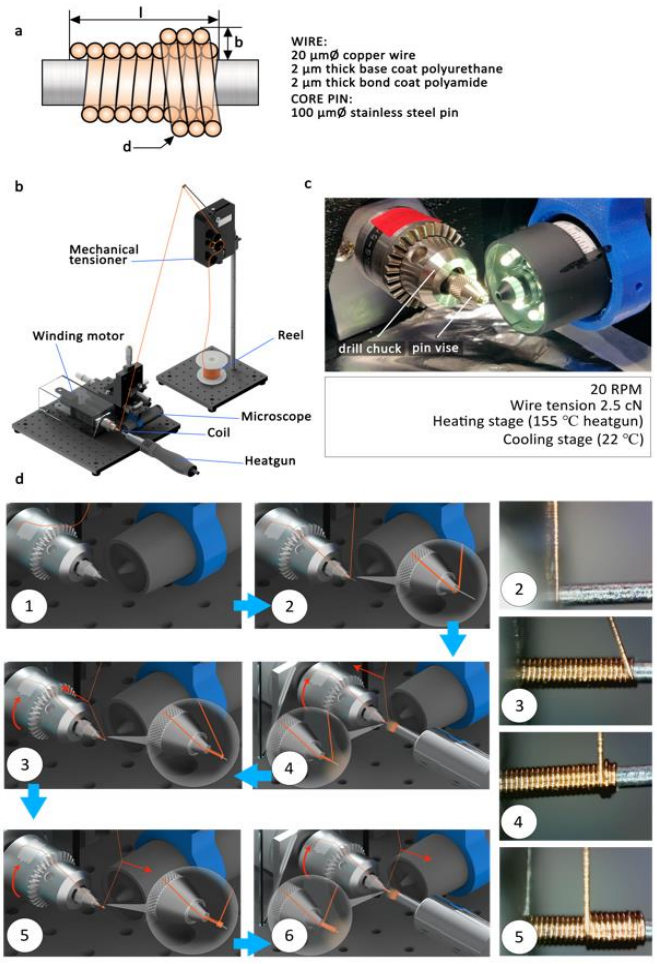

Fig 1. Manufacturing process of the microcoils. (a) Helical winding design of the coil and materials; (b) microwinding machine (c) closeup photograph of the microwinding machine (d) Schematics of the winding process steps (d left), and real microscopic photographs of the results at each step (d right).

The winding motor is a DC motor with a 1:65 reduction gearbox. The cores of the microcoils are attached to the axis by using two consecutive drill chucks, figure 1-c. The minimum diameter of this type of pin vise is virtually zero, this means the inner core can be as small as required. A heat gun for activation of the self-bonding layer is also used and set at 155 °C. The microscope is attached to an XYZ manual displacement stage table. The total cost of all the items is less than 1500€. This method is low-cost and easy to replicate in any lab or small company. The process is very susceptible to full automation since the guiding of the wire, the activation of a heat gun and the rotation activation can easily be

This article has been accepted for publication in IEEE/ASME Transactions on Mechatronics. This is the author's version which has not been fully edited and content may change prior to final publication. Citation information: DOI 10.1109/TMECH.2022.3215233

programmed.

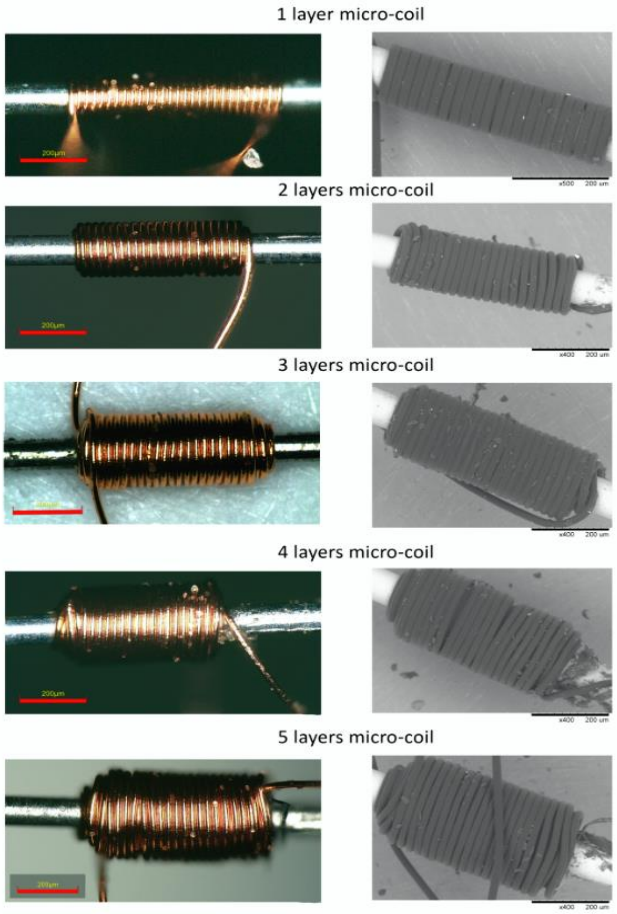

Fig. 2. Manufactured coils with 1 to 5 layers. Digital optical microscopy images (left) and scanning electron microscopy (SEM) images (right).

The manufacturing process is shown, step by step, in Fig 1-d. Step one (1) positioning the inner core in the pin vise. In the second step (2), the wire is wound around the inner core, so the wire acquires the preadjusted tension. Once it is ready, the motor is turned on at a controlled slow rate of approximately 20 rpm, step (3). When the layer is almost completed, 2-3 turns before the end, the heat gun is disconnected. After finishing the first layer, a short pulse of hot air is applied to secure the initial second layer turns, step (4). Then, rotation is activated, and the second layer is completed. During this step, as in step (2), hot air should be applied continuously to ensure adequate adhesion between layers and between the new turns, step (5) and again step (6), which starts again the process.

B. Results and discussion

Several sets of microcoils with different number of layers have been manufactured. Optical microscope and SEM pictures of the microcoils are shown in Fig 2. Microcoils reported in this paper are approximately 550 µm in length, but the minimum length could be down to 24 µm for a single-turn coil. The number of turns per layer is between 20 and 25. The digital microscope allows for an accurate measurement of distances. Fill factors can be calculated using equation (2):

$$F = \frac{\pi d^2 n}{4bl} \quad (2)$$

The results of fill factor as a function of the number of layers are listed in Table I.

The outer diameter is 3 times smaller than the smallest diameter ever achieved by winding techniques while keeping a high fill factor and a large number of layers. Such small and highly performant microcoils have never been demonstrated neither by winding processes nor epitaxial growth techniques. The fill factor is always larger than 76% in any case, and larger than 84% for microcoils with two layers or more. This is a larger fill factor than those found for microcoils produced by deposition techniques, as expected. The fill factors vary from 76% in the one-layer microcoil to 91% in the four-layer microcoil. The fill factor achieved in the proposed technique is high and like the one of macroscopic coils.

TABLE I. GEOMETRY AND FILL FACTOR FOR THE MANUFACTURED MICROCOILS.

Number of layers	**1**	**2**	**3**	**4**	**5**
d, Wire diameter (µm)	24	24	24	24	24
b, Width (µm)	24.5	43	60	83	94
l, Length (µm)	680	527	580	515	577
D, Microcoil outer diameter (µm)	149	186	220	266	288
Number of turns	28	45	65	86	106
Fill factor (%)	76%	90%	84%	91%	88%
Coiling time (s)	180	260	340	420	500
Failure rate (%)	0.5%	0.8%	1%	1.8%	2.5%

III. THERMOELECTRICAL CHARACTERIZATION OF MICROCOILS IN HUMAN-BODY-LIKE ENVIRONMENTS

For medical applications, it is standardized that implantable devices can never have temperatures higher than 43 °C in the areas in contact with tissue. The environment and tissues considered for testing are air, Simulated body fluid (SBF), muscle (pork meat) and fat (pork fat). No additional dissipation has been considered so that the resulting information could be more easily extrapolated to other more complex applications and environments.

A. Theoretical approach

The average temperature increase in the whole system can be estimated by measuring the variation in the electrical resistance produced by Joule's heating effect. The temperature of the microcoils can be accurately determined considering the change in their electrical resistance due to Joule effect heating. Microcoil resistance can be calculated as:

$$R(T) = R_0(1 + \alpha(T - T_0)) \quad (3)$$

where R_0 is the resistance of the coil plus the connection wires (measured at room temperature), α is the temperature coefficient of the copper wire ($\alpha = 3.93 \cdot 10^{-3} \, ^\circ C^{-1}$), T *is* the temperature of the coil and T_0 is the room temperature.

For steady state conditions, power dissipation in the coil can be calculated as:

$$W = V \cdot I = I^2 \cdot R(T) \quad (4)$$

where V is the voltage drop and I is the circulating current in the coil. By combining Eqs. 3 and 4, the average temperature of the coil can be expressed as:

$$T = T_0 + \frac{1}{\alpha} \cdot \left(\frac{V}{IR_0} - 1 \right) \quad (5)$$

B. Experimental setup and procedure

The tests are carried out by applying DC current in controlled steps and measuring the voltage drop between both ends of each microcoil. By measuring the voltage drop and the current, the variation in resistance can be calculated. Coils are powered using a TENMA 72-2705 programmable 90 W DC Power Supply, which can supply DC current in steps of just 1 mA. The current is increased by small and discrete steps, and sufficient time is left between steps to stabilize the temperature and resistance of the coils. The current is increased until coils suddenly break, or a short circuit occurs. Voltage drops at shunt resistance and coils are measured by a 16-bit data acquisition card from National Instruments model USB-6211.

Characterization of the maximum current density and temperature increase is performed in four different human body-like environments: room temperature air, Fig 3-a; muscle tissue (pork meat), Fig 3-c; fat tissue (pork fat), figure 3-b; SBF at 36 °C, Fig 3-c. The elaboration of SBF has followed the recipe published by a Kyoto University team [34]. Once the solution is ready, the microcoil is submerged into the fluid at a controlled temperature of 36±1° for all tests.

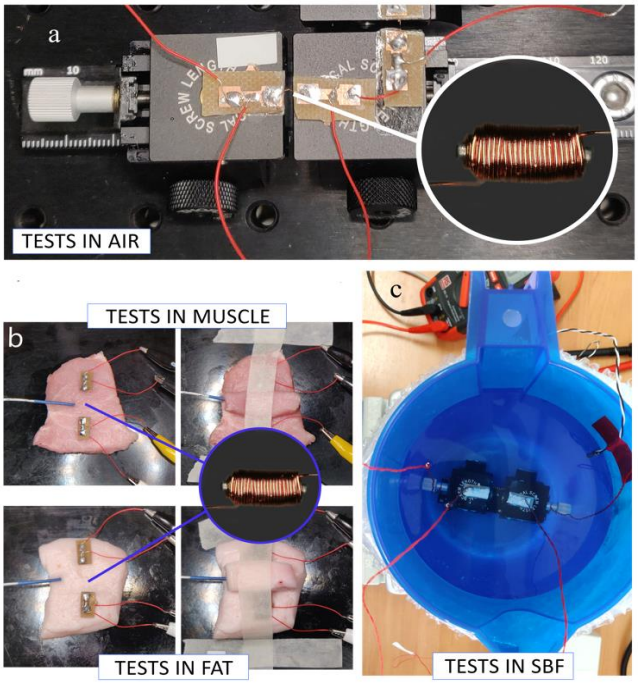

Fig. 3. Experimental setup for determining the thermoelectrical behavior of the microcoil. (a) microcoil ready to be tested in a room-temperature air environment. (b) microcoil during the tests in muscle tissue and fat tissue. (c) Test bench submerged in 36 °C simulated body fluid.

C. Results and discussion

Fig. 4-a shows a test of a 3-layer microcoil in an air environment at room temperature. The current density is increased in steps of 20 A/mm^2 until failure. Coil failure can be clearly observed at time t = 445 s, when coil measured resistance (hence calculated temperature) drops drastically due to an internal short circuit of the coil. All coils fail at a temperature of approximately 250 °C.

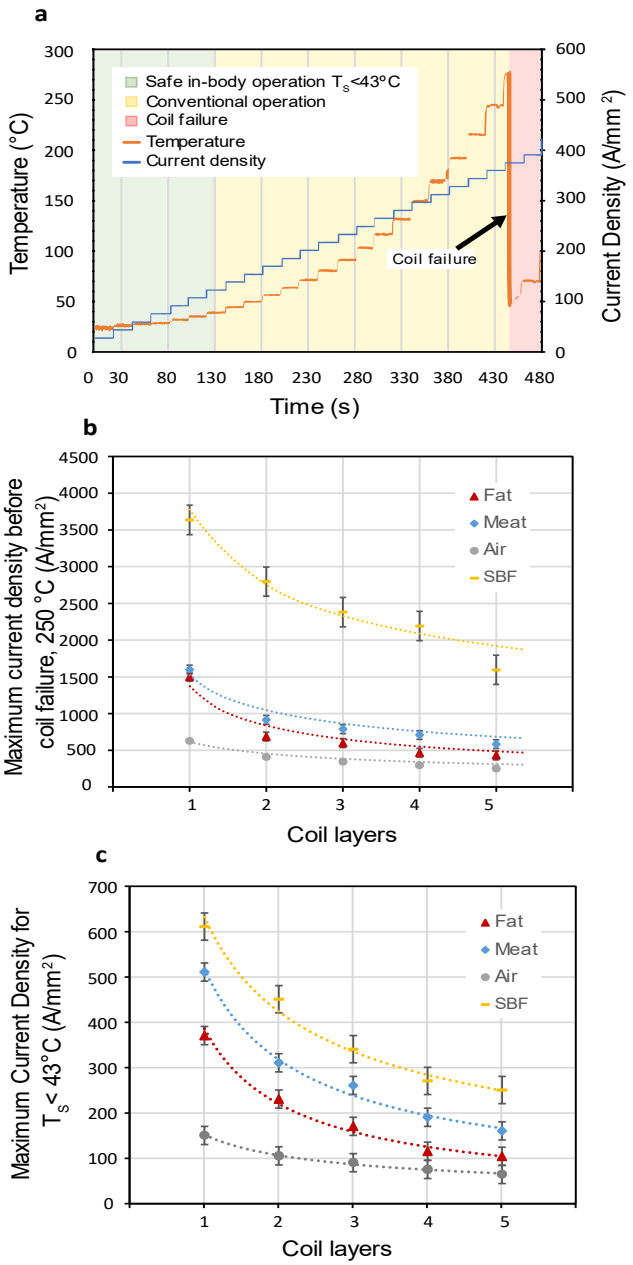

Fig. 4. (a) test for a three-layer microcoil. Coil average temperature vs. current density in air. (b) Maximum current density before coil failure for a different number of layers in different environments. (c) Maximum current density before potential tissue damage (43 °C).

The maximum current density before coil failure for different numbers of layers is shown in Fig 4-b. As the number of layers increases, the maximum current density decreases. Operation in room temperature air presents the lowest current density allowance, which is as low as 250 A/mm^2 for a five-layer coil. Fat and meat tissues are less restrictive than air. Fat allows from 1.6 to 2.5 times more current density with respect to air. Meat allows 2.5-3.4 times more current density with respect to air. The tests performed with the coil immersed in SBF present the largest allowable current density, which is approximately 1600 A/mm^2 for a single-layer microcoil. A maximum current density of 3600 A/mm^2 is measured for a single-layer microcoil inside the SBF. The maximum current density in SBF appears to be 5.8–6.4 times that in air, independent of the number of turns. In all cases, current densities are about 2 orders of magnitude larger than typical current density in macroscale actuators [35].

Fig. 4-c shows the maximum current density in the

microcoil for a surface temperature increase of 7 °C. This corresponds to the maximum temperature increase allowable for a microcoil operating inside the human body, so it does not exceed 43 °C. The maximum current density decays when the number of turns in the coil is increased. Again, operation in air presents the lowest current density allowance, which is as low as 60 A/mm^2 for a five-layer coil and 150 A/mm^2 for a single-layer coil. Similar to the maximum temperature before failure, fat and meat tissues are less restrictive than air. Tests performed with the coil immersed in SBF present the largest allowable current density (Ts<43 °C), which is approximately 610 A/mm^2 for a single-layer microcoil and 250 A/mm^2 for a five-layer microcoil. In all cases, the maximum current densities are inversely proportional to the number of layers. This can be properly explained by a geometric scale effect. Increasing the number of turns increases both the external surface (~r^2) and the volume of the coils (~r^3) while dissipation capacity increases proportionally to the external surface (~r^2).

IV. Conclusions

A clean-room free method for manufacturing multilayered micrometric coils is presented in this work. Microcoil manufacturing is achieved by using a semiautomatic microwinding system. This method has demonstrated the production of multilayered coils tens to hundreds of micrometres long, with outer diameters ranging between 150 and 300 µm, arrangements of up to 5 consecutive layers, and an average fill factor of 85%. This means 3 times smaller diameters than the smallest diameter ever achieved by wire winding. The process is very susceptible to full automation.

The manufactured microcoils have been tested inside different human body-like environments: immersed in static air, inside fat and muscle tissue and immersed in simulated body fluid at 36 °C. A maximum current density before coil failure (Ts~250 °C) of 3600 A/mm^2 was experimentally determined for single layer microcoils immersed in SBF. For microcoils operating inside the human body, their maximum surface temperature shall not exceed 43 °C to prevent potential tissue damage. The test in air presents the lowest current density, which is as low as 60 A/mm^2 for a five-layer coil and 150 A/mm^2 for a single-layer coil. Fat and meat tissues are less restrictive than air. Tests performed with the coil immersed in SBF present the largest allowable current density, which is approximately 250 A/mm^2 for a five-layer microcoil. It is important to highlight that especial design considerations for the current density shall be taken when designing micro actuators, as they can withstand much more current density as demonstrated for the first time in this work.

References

[1] X. Huang, R. Horowitz, and Y. Li, “A comparative study of MEMS microactuators for use in a dual-stage servo with an instrumented suspension,” *IEEE/ASME Trans. Mechatronics*, vol. 11, no. 5, pp. 524–532, Oct. 2006, doi: 10.1109/TMECH.2006.882982.

[2] A. Acemoglu, D. Pucci, and L. S. Mattos, “Design and Control of a Magnetic Laser Scanner for Endoscopic Microsurgeries,” *IEEE/ASME Trans. Mechatronics*, vol. 24, no. 2, pp. 527–537, Apr. 2019, doi: 10.1109/TMECH.2019.2896248.

[3] R. Sriramshankar and G. R. Jayanth, “An Integrated Magnetic Actuation System for High-Speed Atomic Force Microscopy,” *IEEE/ASME Trans. Mechatronics*, vol. 23, no. 5, pp. 2285–2294, 2018, doi: 10.1109/TMECH.2018.2857464.

[4] H. Mei, K. A. Thackston, R. A. Bercich, J. G. R. Jefferys, and P. P. Irazoqui, “Cavity resonator wireless power transfer system for freely moving animal experiments,” *IEEE Trans. Biomed. Eng.*, vol. 64, no. 4, pp. 775–785, Apr. 2017, doi: 10.1109/TBME.2016.2576469.

[5] E. Diez-Jimenez *et al.*, “Magnetic and morphological characterization of Nd2Fe14B magnets with different quality grades at low temperature 5–300 K,” *J. Magn. Magn. Mater.*, vol. 451, 2018, doi: 10.1016/j.jmmm.2017.11.109.

[6] E. Diez-Jimenez, C. Alén-Cordero, R. Alcover-Sánchez, and E. Corral-Abad, “Modelling and test of an integrated magnetic spring-eddy current damper for space applications,” *Actuators*, vol. 10, no. 1, pp. 1–18, 2021, doi: 10.3390/act10010008.

[7] J. Gao *et al.*, “Design and Testing of a Motor-Based Capsule Robot Powered by Wireless Power Transmission,” *IEEE/ASME Trans. Mechatronics*, vol. 21, no. 2, pp. 683–693, 2016, doi: 10.1109/TMECH.2015.2497083.

[8] K. Gosalia, M. S. Humayun, and G. Lazzi, “Impedance matching and implementation of planar space-filling dipoles as intraocular implanted antennas in a retinal prosthesis,” *IEEE Trans. Antennas Propag.*, vol. 53, no. 8 I, pp. 2365–2373, Aug. 2005, doi: 10.1109/TAP.2005.852514.

[9] M. Mohmmadzadeh *et al.*, “Characterization of a 3D MEMS fabricated micro-solenoid at 9.4 T,” *J. Magn. Reson.*, vol. 208, no. 1, pp. 20–26, 2011, doi: 10.1016/j.jmr.2010.09.021.

[10] K. T. Nguyen, B. Kang, E. Choi, J. O. Park, and C. S. Kim, “High-Frequency and High-Powered Electromagnetic Actuation System Utilizing Two-Stage Resonant Effects,” *IEEE/ASME Trans. Mechatronics*, vol. 25, no. 5, pp. 2398–2408, Oct. 2020, doi: 10.1109/TMECH.2020.2974069.

[11] D. D. Karnaushenko, D. Karnaushenko, D. Makarov, and O. G. Schmidt, “Compact helical antenna for smart implant applications,” *NPG Asia Mater.*, vol. 7, no. 6, p. 188, Jun. 2015, doi: 10.1038/am.2015.53.

[12] J. Gao and G. Yan, “A novel power management circuit using a super-capacitor array for wireless powered capsule robot,” *IEEE/ASME Trans. Mechatronics*, vol. 22, no. 3, pp. 1444–1455, Jun. 2017, doi: 10.1109/TMECH.2016.2646859.

[13] P. Basset, A. Kaiser, B. Legrand, D. Collard, and L. Buchaillot, “Complete system for wireless powering and remote control of electrostatic actuators by inductive coupling,” *IEEE/ASME Trans. Mechatronics*, vol. 12, no. 1, pp. 23–31, Feb. 2007, doi: 10.1109/TMECH.2006.886245.

[14] Z. Yang, L. Yang, and L. Zhang, “Autonomous Navigation of Magnetic Microrobots in a Large Workspace Using Mobile-Coil System,” *IEEE/ASME Trans. Mechatronics*, vol. 26, no. 6, pp. 3163–3174, Dec. 2021, doi: 10.1109/TMECH.2021.3054927.

[15] A. Hajiaghajani, D. Kim, A. Abdolali, and S. Ahn, “Patterned Magnetic Fields for Remote Steering and Wireless Powering to a Swimming Microrobot,” *IEEE/ASME Trans. Mechatronics*, vol. 25, no. 1, pp. 207–216, Feb. 2020, doi: 10.1109/TMECH.2019.2951101.

[16] T. Kato, F. King, K. Takagi, and N. Hata, “Robotized Catheter with Enhanced Distal Targeting for Peripheral Pulmonary Biopsy,” *IEEE/ASME Trans. Mechatronics*, vol. 26, no. 5, pp. 2451–2461, Oct. 2021, doi: 10.1109/TMECH.2020.3040314.

[17] G. Li, N. A. Patel, E. C. Burdette, J. G. Pilitsis, H. Su, and G. S. Fischer, “A Fully Actuated Robotic Assistant for MRI-Guided Precision Conformal Ablation of Brain Tumors,” *IEEE/ASME Trans. Mechatronics*, vol. 26, no. 1, pp. 255–266, Feb. 2021, doi: 10.1109/TMECH.2020.3012903.

[18] J. A. Martínez Rojas, J. L. Fernández, R. S. Montero, P. L. L. Espí, and E. Diez-Jimenez, “Model-based systems engineering applied to trade-off analysis of wireless power transfer technologies for implanted biomedical microdevices,” *Sensors*, vol. 21, no. 9, 2021, doi: 10.3390/s21093201.

[19] M. Martinez-Muñoz, E. DIez-Jimenez, R. Sanchez-Montero, P. L. Lopez-Espi, and J. A. Martinez-Rojas, “Analysis of the geometric parameters influence in PCB fixtures for 2D multipole magnetization patterning of thin layer micro-magnets,” *Int. J. Appl. Electromagn. Mech.*, vol. 61, no. 1, pp. 59–71, 2019, doi: 10.3233/JAE-180121.

[20] M. Martinez-Muñoz, E. Diez-Jimenez, G. V. Villalba-Alumbreros, M. Michalowski, and A. Lastra-Sedano,

"Geometrical dependence in fixtures for 2D multipole micromagnets magnetization pattering," *Appl. Comput. Electromagn. Soc. J.*, vol. 34, no. 7, 2019.

[21] T. Kohlmeier, V. Seidemann, S. Büttgenbach, and H. H. Gatzen, "An investigation on technologies to fabricate microcoils for miniaturized actuator systems," *Microsyst. Technol.*, vol. 10, no. 3, pp. 175–181, 2004, doi: 10.1007/s00542-003-0362-3.

[22] M. Amato, F. Dalena, C. Coviello, M. De Vittorio, and S. Petroni, "Modeling, fabrication and characterization of micro-coils as magnetic inductors for wireless power transfer," *Microelectron. Eng.*, vol. 111, pp. 143–148, 2013, doi: 10.1016/j.mee.2013.03.038.

[23] Z. Feng, S. Zhi, M. Wei, Y. Zhou, C. Liu, and C. Lei, "An integrated three-dimensional micro-solenoid giant magnetoimpedance sensing system based on MEMS technology," *Sensors Actuators, A Phys.*, vol. 299, p. 111640, 2019, doi: 10.1016/j.sna.2019.111640.

[24] H. Ota, T. Oda, and M. Kobayashi, "Development of coil winding process for radial gap type electromagnetic micro-rotating machine," *Proc. IEEE Micro Electro Mech. Syst.*, pp. 197–202, 1995, doi: 10.1109/memsys.1995.472580.

[25] J. Klein and H. Guckel, "High winding density micro coils for magnetic actuators," *Microsyst. Technol.*, vol. 4, no. 4, pp. 172–175, 1998, doi: 10.1007/s005420050124.

[26] Benatav, "Benatav: White Paper on Ultra-Fine Wire Technologies in Medical Devices," 2021. https://benatav.com/wp-content/uploads/2016/11/white-paper.pdf (accessed Sep. 23, 2021).

[27] Audemars, "Audemars Custom Micro Coil Solutions Information," 2021. https://audemars.com/micro-coils-manufacturing/ (accessed Sep. 23, 2021).

[28] S. Uchiyama *et al.*, "Novel MEMS-based fabrication technology of micro solenoid-type inductor," *J. Micromechanics Microengineering*, vol. 23, no. 11, 2013, doi: 10.1088/0960-1317/23/11/114009.

[29] S. Y. Wu, C. Yang, W. Hsu, and L. Lin, "3D-printed microelectronics for integrated circuitry and passive wireless sensors," *Microsystems Nanoeng.*, vol. 1, no. April, pp. 1–9, 2015, doi: 10.1038/micronano.2015.13.

[30] L. Hirt, A. Reiser, R. Spolenak, and T. Zambelli, "Additive Manufacturing of Metal Structures at the Micrometer Scale," *Adv. Mater.*, vol. 29, no. 17, p. 1604211, May 2017, doi: 10.1002/ADMA.201604211.

[31] J. Moulin, M. Woytasik, J. P. Grandchamp, E. Dufour-Gergam, and A. Bosseboeuf, "High current densities in copper microcoils: influence of substrate on failure mode," *Microsyst. Technol.*, vol. 13, no. 11–12, pp. 1553–1558, 2007, doi: 10.1007/s00542-007-0391-4.

[32] T. Zhang, P. Zhang, H. wen Li, Y. hui Wu, and Y. shun Liu, "Fabrication of micro electromagnetic actuator of high energy density," *Mater. Chem. Phys.*, vol. 108, no. 2–3, pp. 325–330, 2008, doi: 10.1016/j.matchemphys.2007.09.046.

[33] P. S. Yarmolenko *et al.*, "Thresholds for thermal damage to normal tissues: An update," *Int. J. Hyperth.*, vol. 27, no. 4, pp. 320–343, Jun. 2011, doi: 10.3109/02656736.2010.534527.

[34] A. Oyane, H. M. Kim, T. Furuya, T. Kokubo, T. Miyazaki, and T. Nakamura, "Preparation and assessment of revised simulated body fluids," *J. Biomed. Mater. Res. - Part A*, vol. 65, no. 2, pp. 188–195, 2003, doi: 10.1002/jbm.a.10482.

[35] D. Hanselman, "Brushless Permanent Magnet Motor Design Second Edition," *Magna Phys. Publ.*, vol. 2, p. 392, 2006, Accessed: Nov. 07, 2021. [Online]. Available: www.eece.maine.edu.

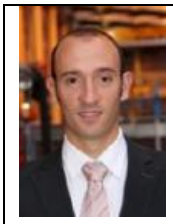

Efrén Díez Jiménez is Associate Professor at Mechanical Engineering area of Universidad de Alcalá. He obtained his PhD on Mechanical Engineering and Industrial Organization in 2012. His main research interests are MEMS, microactuators and magnetic devices.

Ignacio Valiente Blanco is working in the mechanical Area of University of Alcala supported by a Ramón y Cajal Research Grant. His research interests are focused in magnetismand renewable energies.

Gabriel Villalba Alumbreros received his BSc in Electronics and Industrial Automation Engineering in 2019. His research interests are focused in electromagnetic actuators, mechatronic systems, MEMS and control systems.

Miguel Fernández Muñoz received his Bachelor Degree in Electronic and Automation Engineering from University of Alcala in 2019. His main research interests are micro systems and personal rapid transport systems.

Diego Lopez Pascual received his MsC on Industrial Engineering in 2020 by Universidad de Alcalá. His research interests are micromotors, renewable energy systems and MEMS.

Alberto Lastra has a Ph.D. in Mathematics by the University of Valladolid. He is associate professor at the Universidad de Alcalá (Spain). His research interests are asymptotic analysis of functional equations in the complex domain and related topics, symbolic computation, or orthogonal polynomials.

Carlos Morón Alguacil received his MSc in Industrial Engineering in 2019. His main research interests are mechatronic systems and mechanism prototyping.

Alba Martínez Pérez is graphic designer and laboratory assistant in UWIPOM2 project. Her main research interests are mechatronic systems, graphical design and mechanism prototyping.